THM113 SWARM-EX

Mathematical Thermal Analysis

Table of Contents

Abbreviation

ADCS = Attitude and Determination Control System
CDH = Command and Data Handling
COM = Communications
ConOps = Concept of Operations
EPS = Electrical Power Systems
ICD = Interface Control Document
INST = Instrument
IR = Infrared Heat Flux
ISS = International Space Station
LASP = Laboratory for Atmospheric and Space Physics
MAXWELL = Multiple Access X-band Wave Experiment Located in LEO
MCU = Microcontroller
MinXSS = Miniature X-ray Solar Spectrometer
PCB = Printed Circuit Board
SCI = Science Team
STR = Structures
LEO = Low Earth Orbit
SWARM-EX = Space Weather Atmospheric Reconfigurable Multiscale Experiement
TBAL = Thermal Balance
TCS = Thermal Control System
TD = Thermal Desktop
TVAC = Thermal Vacuum
UHF = Ultra High Frequency

Nomenclature

A = Area
a = Semi-major axis of the satellite orbit
α = Absorptivity
β = Angle of the orbit plane with respect to the solar vector
C = Corrected Sun position
c_p = Specific heat capacity
δ = Solar declination
e = Eccentricity of an orbit
ϵ = Earth's axis tilt
ε = Emissivity

F = Optical view factor
G = Universal gravitational constant
Γ = True solar longitude
h = Spacecraft altitude from the Earth's surface
I = Current
i = Inclination angle of the orbit plane with respect to the Earth equatorial plane
J_2 = Coefficient of Earth's oblateness in orbital mechanics
k = Thermal conductivity
L_0 = Mean longitude of the Sun
l = Length
M = Mass of the Earth
M = Mean anomaly of the Sun
m = Mass of an object
μ = Earth's gravitational parameter
Ω_0 = Initial right ascension of the ascending node
Q = Heat energy
q = Energy per area unit
r_{earth} = Radius of the Earth
ρ = Density
σ = Botzman's constant
t = Time
T = Temperature
V = Voltage

I. Introduction

The purpose of this document is to develop thermal mathematical models to predict system- and component-level temperature variation profiles, and to validate the existing Thermal Desktop (TD) thermal model. Building these models is an important step to verify the reliability and accuracy of the numerical solutions before conducting experimental simulations in a thermal vacuum (TVAC).

an unexpected delay in the TD license renewal, combined with serious technical issues. Given these circumstances, it was a good opportunity to deepen the understanding of spacecraft temperature modeling and to refine prediction accuracy. The overall objective of the analyses is to establish a theoretical understanding of the maximum and minimum temperature ranges for each component under selected worst-case scenario conditions, considering both steady and time-dependent states.

II. Analytical Methods

In order to develop analytical models for the steady state, space environmental impacts on spacecraft need to be understood and defined for the worst case scenarios conditions such as hot and cold cases. The SWARM-EX 3U CubeSat is expected to launch in an inclination of 52 deg (same as ISS orbit) or 90 deg (polar orbit) in March 2026, operating for a period of 4.25 years. The orbit should be circular (e = 0) at an altitude of 480 km above the Earth surface.

Orbital Parameter	Altitude h [km]	Eccentricity e	Inclination i [deg]	Target Launch Date	Duration [year]
Value	480	0	52/90	March 2026	4.25

Table 1. Target Orbital Parameters

A. Orbit Time

To begin with, it is important to identify the whole orbit time and the orbit time in eclipse under the conditions shown in table 2. Based on the analysis, the beta angle, the angle of the orbit plane related to the sun vector, for the cold and hot case scenarios can be determined. The orbit time period was calculated, using Kepler's 3rd Law. To recall the 3rd Law, it states that "the square of the period, T of a planet or spacecraft is proportional to the cube of its mean distance, a to the sun or its central body." (Rickman) The mathematical expression is shown below.

$$T^2 \propto a^3$$

$$T^2 = \frac{4\pi^2}{GM} a^3$$

G is the universal gravitational constant. M is the mass of the central body, Earth, for this mission. The mean distance, a is defined as the distance of the satellite from the center of the planet ($a = r_{earth} + h$) for the circular orbit (e = 0). h is the altitude of the spacecraft.

Constant	G [$km^3/kg \cdot s^2$]	M [kg]	r_{earth} [km]
Value	6.6743E-20	5.9722E24	6378

Table 2. Constants for Kepler's 3rd Law

Using Kepler's 3rd law, the total orbit time period is 94.2 min per orbit. In addition, it is also important to know how long the spacecraft experiences the eclipse during the orbit. In order to calculate it, it needs to determine the variation of the beta angle throughout the mission first because the eclipse time is dependent on the beta angle. First, it is assumed that the eclipse occurs within the umbral region, where sunlight is completely blocked. For reference, the penumbral region is where sunlight is only partially obscured. The figure below briefly describes the two regions. (Rickman)

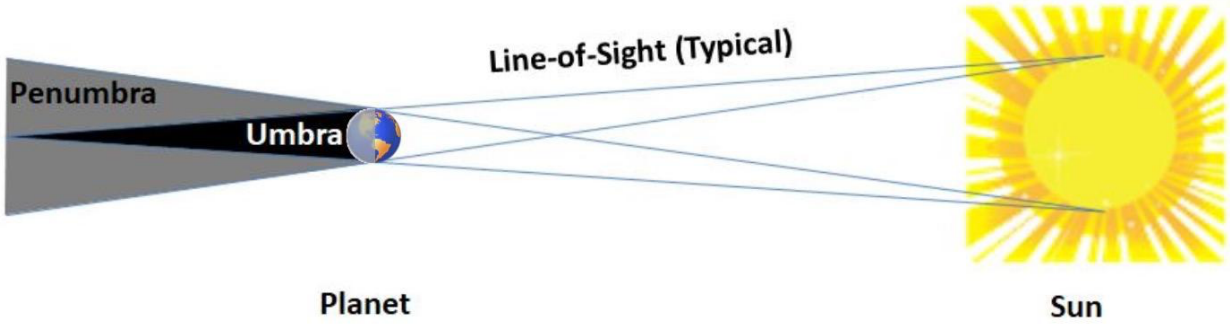

Figure 1. Definition of Penumbra and Umbra Regions

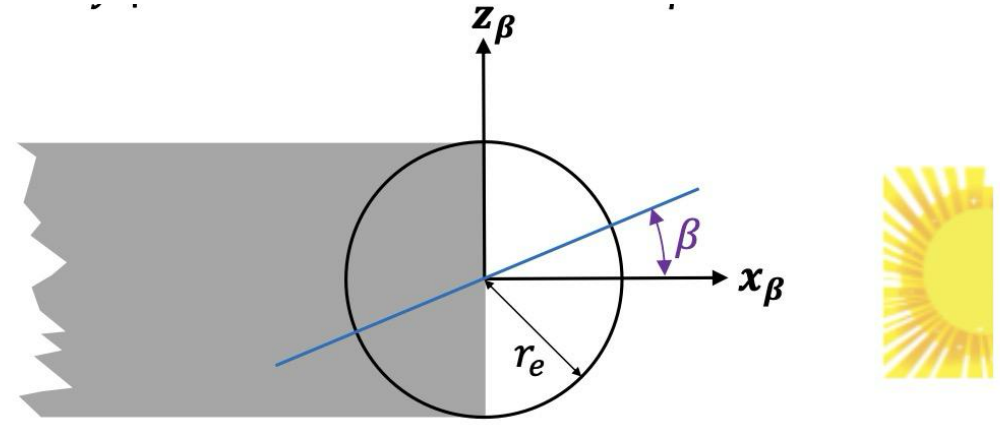

(a) x-z Coordinates of the β-plane

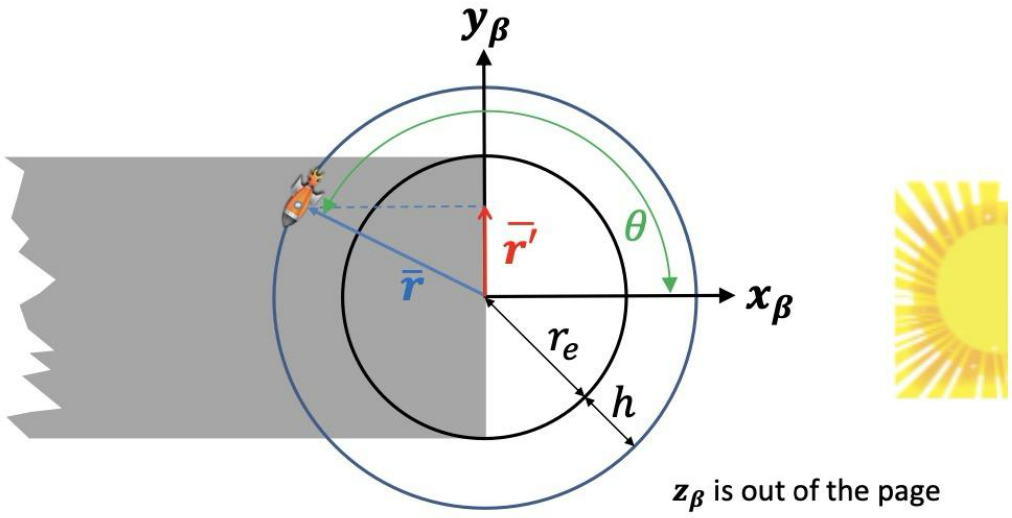

(b) x-y Coordinates of the β-plane

Figure 2. Relationship between Eclipse and Beta Angle

Figure 1 indicates the relationship between the eclipse and the beta angle, which helps to determine the fraction of orbit spent in eclipse for a LEO circular orbit with respect to the beta

angle. (Rickman) As figure 2 shows, the critical beta angle can be defined as below. It indicates that at any beta angle above the critical angle, the spacecraft experiences no eclipse at all.

$$\beta_{critical} = sin^{-1}\left(\frac{r_{earth}}{a}\right)$$

Then, the fraction of orbit spent in eclipse can be expressed as a function of β as follows:

$$f(\beta) \quad = \frac{1}{\pi} cos^{-1}\left(\frac{\sqrt{h^2 + 2r_{earth}h}}{a \cdot cos(\beta)}\right)$$

Taking into account the calculated eclipse fraction of the orbit over β, the maximum orbit time in eclipse occurs at β = 0˚ for 35.8 mins. In contrast, no eclipse occurs at any β angle above 68.4˚ under the target launch parameters. Figure 3 below indicates the results of the orbit spent in sunlight and eclipse.

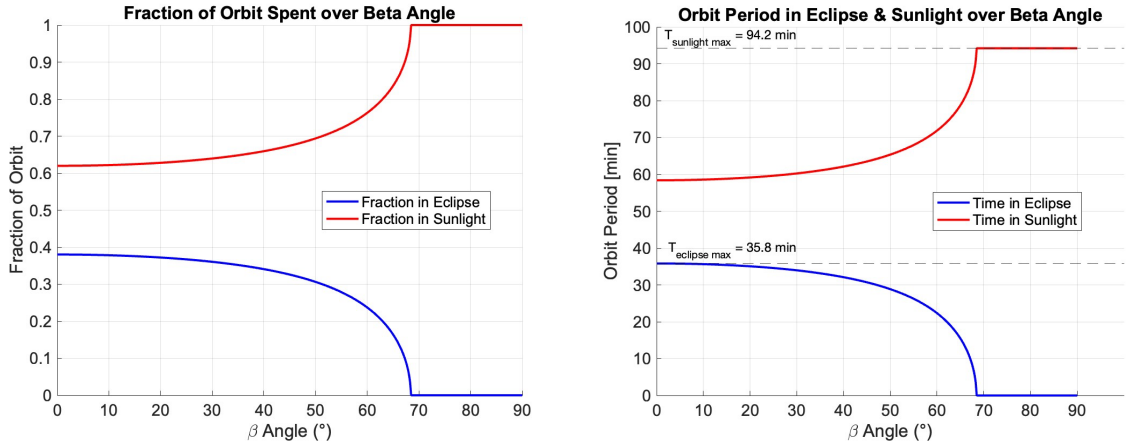

Fig 3. Orbit Time Spent in Sunlight and Eclipse with a Variation of β

Orbit Time [min]	94.2
Maximum Eclipse Time [min]	35.8 (at β = 0˚)
Minimum Eclipse Time [min]	0 (at β > 68.4˚)

Table 3. Total Orbit Time and Eclipse Times

B. Beta Angle

Now, the maximum and minimum beta angles need to be considered because the variation of β provides a variety of thermal environments for an orbiting spacecraft. The definition of the beta angle is the angle of the orbit plane with respect to the solar vector. This indicates that the beta angle varies over solar orbiting time. When calculating the angle, there are 4 factors that need to be considered, which are the ecliptic true solar longitude Γ, the tilt of the Earth ϵ (the obliquity of the ecliptic), the spacecraft orbit inclination, and the RAAN procession Ω. (Rickman)

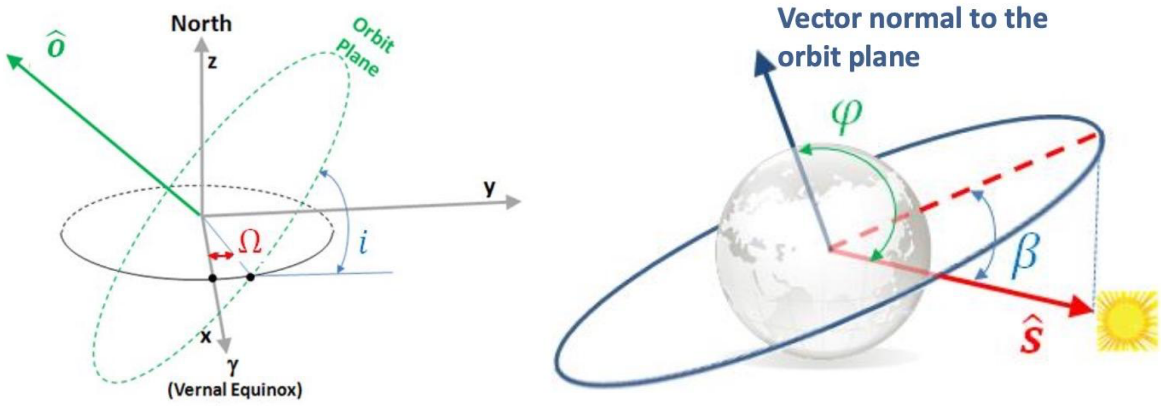

Figure 4. Geometric Relationship of β

First, the mission time needs to be defined in the Julian date for precision. (Square) The time (days) in Julian centuries since J2000 is used as defined below.

$$T = \frac{JD - 2451545}{36525}$$

JD is the MATLAB function of juliandate(launch date).

Next, the RAAN procession over time is determined due to the change in beta angle as the change in ascension angle, which is mathematically described below.

$$\Omega(t) = \Omega_0 + \frac{d\Omega}{dt} \times t$$

$$\frac{d\Omega}{dt} = -\frac{3}{2} J_2 \left(\frac{r_{earth}}{a}\right)^2 \sqrt{\frac{\mu}{a^3}} cos(i)$$

Ω_0 is the initial right ascension of the ascending node, which is 45 deg. J_2 is the coefficient of Earth's oblateness in orbital mechanics (This refers to that Earth is not a perfect sphere). μ is Earth's gravitational parameter.

Ω_0 [deg]	J_2	μ $[km^3/s^2]$
45	1.08263E-3	3.986E5

Table 4. Constants for RAAN Procession

Then, the true solar longitude Γ can be determined, corresponding to the Sun's position. The geometric parameters related to the Sun's position are calculated as follows:

$$\Gamma = L_0 + C$$

$$L_0 = 280.46646 + 36000.76983T$$

$$C = (1.9146 - 0.004817T)sin(M) + (0.01993 - 0.000101T)sin(2M) + 0.00029sin(3M)$$

$$M = 357.52911 + 35999.05029T - 0.0001537 \times T^2$$

L_0 is the mean longitude of the Sun. M is the mean anomaly of the Sun. C is the corrected Sun's position from M due to the Earth's elliptical orbit around the Sun.

Finally, the beta angle over time can be computed as:

$$\beta(t) = sin^{-1}(sin(\delta)cos(i) - cos(\delta)sin(i)sin(\Omega(t)))$$

$$\delta = sin^{-1}(sin(\epsilon)sin(L_0))$$

δ is the solar declination. ϵ is the Earth's tilt axis, which is 23.44 deg.

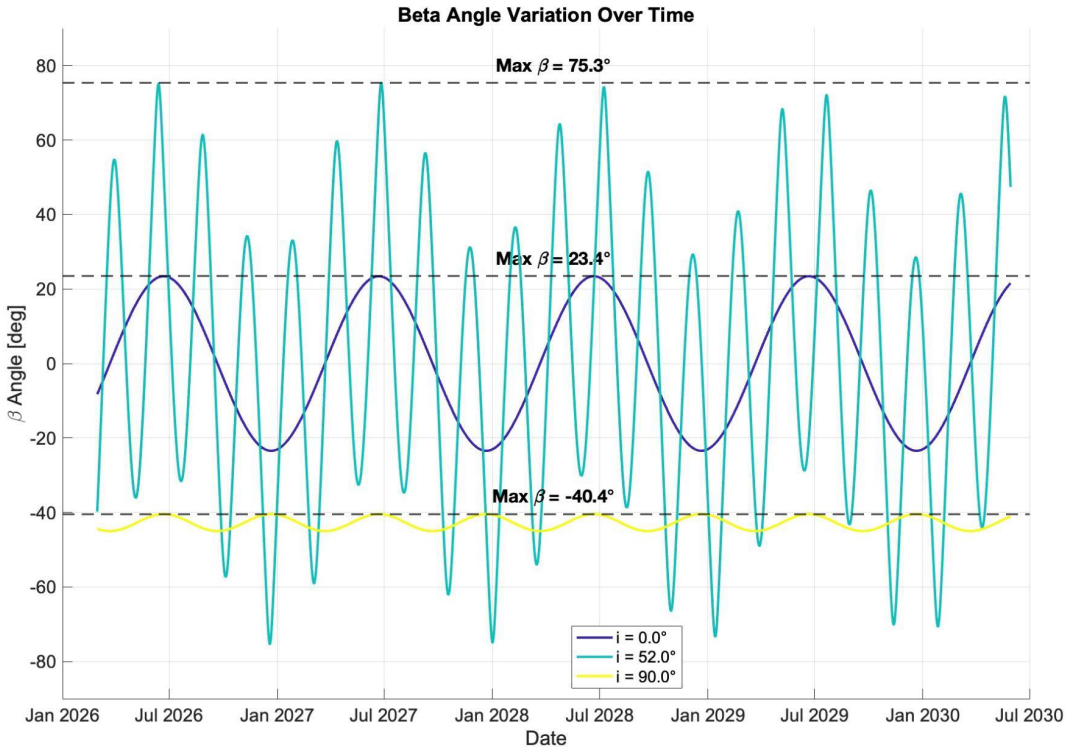

Figure 5. Beta Angle Variation during SWARM-EX Mission

As a result, the maximum beta angle over the full mission duration is 75.3° at an inclination of 52°, indicating that the spacecraft will experience its hottest conditions since it will be continuously exposed to the Sun. On the other hand, the minimum beta angle is 0˚, showing that the spacecraft will be in eclipse the longest for 35.8 min. Table 5. highlights the hot and cold cases based on the previous results.

	Hot Case	**Cold Case**
β [deg]	75.3	0
Eclipse Time [min]	0	35.8

Table 5. Hot and Cold Case Definitions

C. Spacecraft Temperature Derivations

The thermal model of the SWARM-EX satellite is primarily designed for passive thermal control, with the exception of a battery heater. Operational and survival temperatures are maintained through surface coatings, spacecraft orientation, and structural configuration, supported by detailed analysis using TD. At present, the battery heater is the only actively controlled heat source, while other heat-generating components include electrical systems such as PCBs, ADCS, radios, and other subsystems. Figure 6 illustrates the satellite's thermal system.

For the spacecraft's thermal analysis, two primary modes of heat transfer are considered: radiation and conduction. Heat is dissipated into deep space primarily through the spacecraft's main structure, which also functions as a radiator. The structure is made of anodized Al6061 aluminum, with a surface emissivity of 0.88 and an absorptivity of 0.09. In this analysis, the solar panels are excluded from heat transfer considerations, as they are designed to tolerate extreme temperature conditions, and the heat conduction through the panel hinges is determined to be negligibly small.

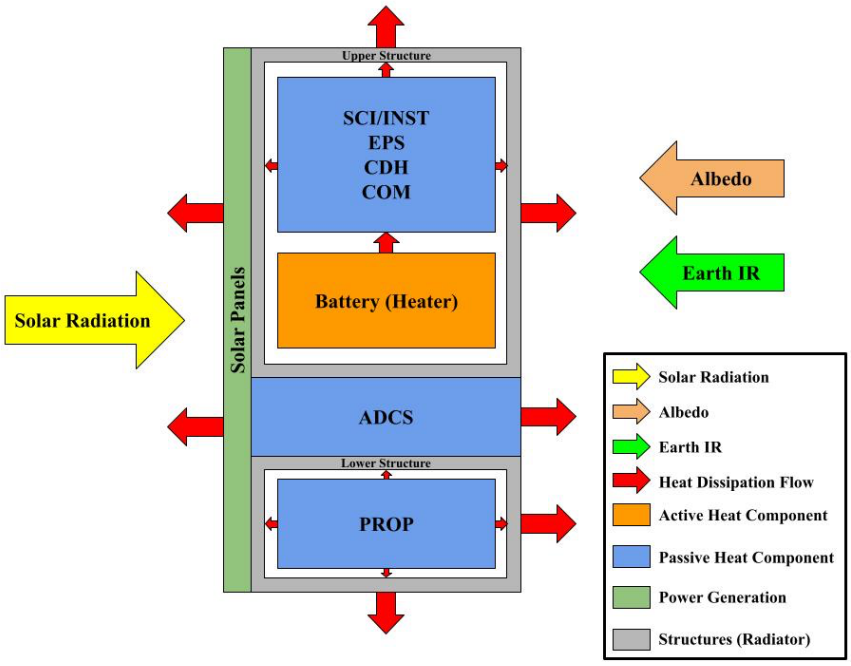

Figure 6. Thermal System Diagram

It is also assumed that heat is distributed equally and uniformly throughout the spacecraft, and that the battery heater remains deactivated. Additionally, the solar flux, albedo flux (reflected radiation from the Earth's surface), and Earth's IR flux are treated as constants. However, each thermal scenario uses different constant values. For example, the solar flux is set to 1414 W/m^2 for the hot case and 1324 W/m^2 for the cold case, based on the variation in Earth's mean distance from the Sun over time. This variation in solar flux can be calculated using Kepler's

First Law. Correspondingly, the albedo flux is adjusted relative to changes in solar flux. Furthermore, the maximum and minimum nominal power generated by the electrical components are determined using the power budgets provided by EPS100. Table 6 summarizes all constants used in the steady-state analysis.

	Hot Case	**Cold Case**
Solar Flux $[W/m^2]$	1414	1324
Albedo Flux $[W/m^2]$	$0.7q_{solar}$	$0.3q_{solar}$
Planet IR Flux $[W/m^2]$	265	208
Nominal Generated Power [W]	30	5

Table 6. Constants for Thermal Analysis in the Steady State

1. Steady State Body Surface Temperature

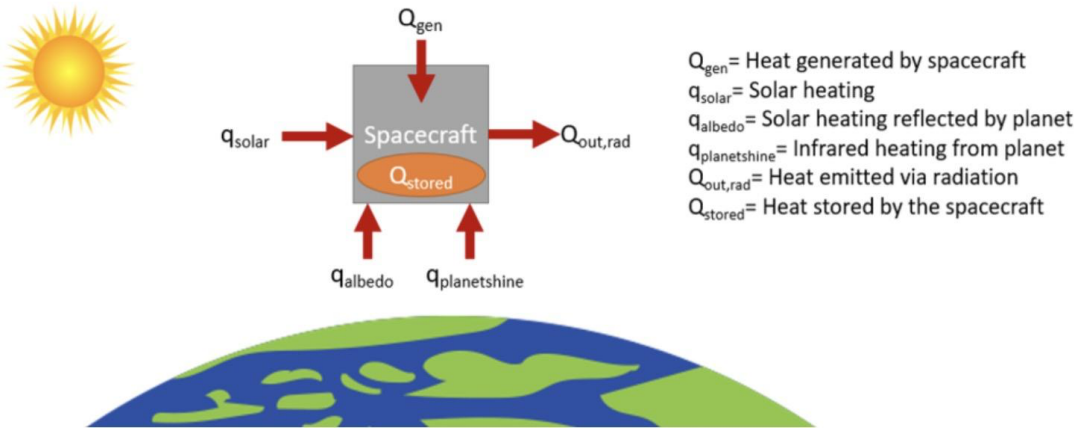

Figure 7. Thermal Equilibrium Diagram

In this section, the body surface temperatures under worst-case scenarios are computed under steady-state conditions, based on the First Law of Thermodynamics, which states the principle of energy conservation, as illustrated in Figure 7. (NASA) The primary input heat sources considered are direct solar radiation, albedo, IR radiation from Earth, and internally generated electrical power. Taking these into account, the energy balance equation is expressed as follows:

$$Q_{in} = Q_{out}$$

$$Q_{solar} + Q_{albedo} + Q_{IR} + Q_{internal} = Q_{out,rad} + Q_{stored}$$

$$\alpha F_s A_s q_s + \alpha F_a A_a q_a + \alpha F_E A_E q_{IR} + \sum_i^n I_i V_i = \sigma \varepsilon F A_{rad}(T^4 - T_s^4) + \sum_i^n m_i c_{p,i}(\frac{dT}{dt})_i$$

T_s is the outer temperature in space, assumed to be 3 K. F is the view factor, assumed to be 0.5.

Since a steady-state condition is assumed, the energy storage term (representing thermal inertia) is neglected, simplifying the energy balance to:

$$\alpha F_s A_s q_s + \alpha F_a A_a q_a + \alpha F_E A_E q_{IR} + \sum_i^n I_i V_i = \sigma \varepsilon F A_{rad}(T^4 - T_s^4)$$

It is further assumed that the solar flux, albedo flux, and Earth's IR flux are incident perpendicular to the body surfaces, maximizing the heat input for a conservative worst-case analysis.

From the equation above, the steady-state surface temperature can be solved.

$$T = \left(\frac{Q_{in}}{\sigma \varepsilon F A_{rad}} + {T_s}^4\right)^{1/4}$$

2. Steady State Component Temperature

In this section, we estimate the steady-state temperatures of internal spacecraft components using the heat flow path diagram shown in Figure 8 (2D Upper Structure). The analysis is based on a steady-state thermal model, where all components are assumed to reach thermal equilibrium without any transient effects.

Assumptions:

- All calculations assume a steady-state condition (no time variation in temperature).
- Components are thermally connected to the main structure using:
  - Stainless steel screws/fasteners, and
  - Direct surface contact (modeled using conservative thermal contact conductance values per NASA/MIL-HDBK).
- The structure radiates heat to deep space at 3 K via a view factor of 0.2-0.3.
- Inter-component radiative exchange is considered via view factors.
- Each component dissipates internal heat due to electrical operation (from the EPS power budget).
- Material-specific properties (e.g., emissivity ε, absorptivity α) are considered for radiative exchange.
- The external surface of the structure is assumed to be at the steady-state temperatures calculated in Section II.C.1:
  Hot Case: 70.2°C, Cold Case: −56.4°C

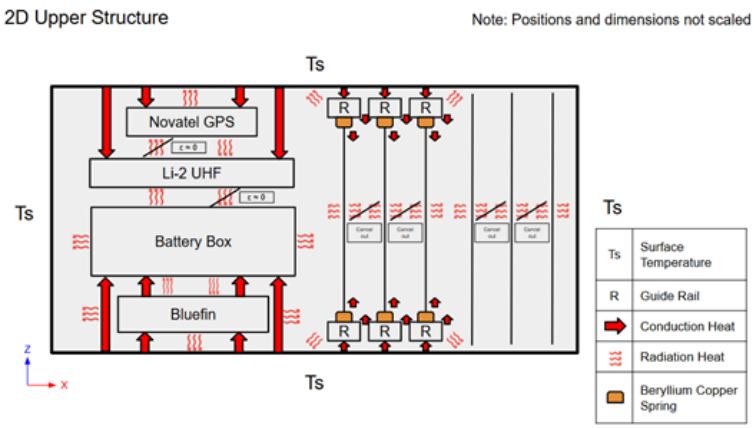

Figure 8. 2D upper structure heat flow path

Thermal Modeling Methodology:

For each component, we apply the First Law of Thermodynamics (energy conservation) at steady state:

$$Q_{in} = Q_{out}$$

$$Q_{Cond} + Q_{internal} = Q_{out,rad}$$

Where:

Q_{in} = Internal power generated by the component (from EPS power budget). Q_{cond} = Heat conducted away via mechanical contacts (screws and surfaces) from structure or from other components. Q_{rad} = Heat radiated to deep space and also heat radiated to neighbouring components

Conduction Modeling:

The conductive heat transfer is modeled as:

For screw conduction: In this analysis, bolted mechanical interfaces between components and the main structure were modeled using thermal conductance values based on screw size and interface type. This approach aligns the analytical model with the physical connections used in the spacecraft CAD. The total thermal conductance of a bolted joint is computed as the product of: The per-screw conductance (from the table below), and The number of screws used for that interface.These values are taken from the *Spacecraft Thermal Control Handbook: Fundamental Technologies* and represent conservative estimates for use in spacecraft thermal modeling.

Screw Size	Conductance (W/K) Small Stiff Surfaces	Conductance (W/K) Large Stiff Surfaces
2-56	0.21	0.105
4-40	0.26	0.132
6-32	0.42	0.176
8-32	0.80	0.264
10-32	1.32	0.527
¼-28	3.51	1.054

Table 7. Conductance for Screws

For surface contact, conservative contact conductance values were used, such as 11000 W/m²·K depending on material and contact pressure.

Thermal contact conductance of some metal surfaces in air (from various sources)

Material	Surface condition	Roughness, μm	Temperature, °C	Pressure, MPa	h_c,* W/m²·K
Identical Metal Pairs					
416 Stainless steel	Ground	2.54	90–200	0.17–2.5	3800
304 Stainless steel	Ground	1.14	20	4–7	1900
Aluminum	Ground	2.54	150	1.2–2.5	11,400
Copper	Ground	1.27	20	1.2–20	143,000
Copper	Milled	3.81	20	1–5	55,500
Copper (vacuum)	Milled	0.25	30	0.17–7	11,400
Dissimilar Metal Pairs					
Stainless steel–Aluminum		20–30	20	10 20	2900 3600
Stainless steel–Aluminum		1.0–2.0	20	10 20	16,400 20,800
Steel Ct-30–Aluminum	Ground	1.4–2.0	20	10 15–35	50,000 59,000
Steel Ct-30–Aluminum	Milled	4.5–7.2	20	10 30	4800 8300
Aluminum–Copper	Ground	1.17–1.4	20	5 15	42,000 56,000
Aluminum–Copper	Milled	4.4–4.5	20	10 20–35	12,000 22,000

Figure 9. Thermal Contact Conductance

Radiative Modeling:

The radiation heat loss from a component to space was modeled using the Stefan-Boltzmann Law:

$$\sigma \varepsilon F A_{rad} (T^4 - T_s^4)$$

Where:

- ϵ = emissivity of the component, alpha = absorptivity
- σ = 5.67×10E−8 $W/m^2/K^4$ = Stefan-Boltzmann constant
- A = surface area of the component
- T_s = 3K (deep space temperature)
- F = view factor

Final Temperature Estimation:The steady-state component temperature was found by solving the energy balance equation iteratively for each case (Hot and Cold). The results are summarized in Section IV.B (Results).

3. Time-Dependent Body Surface Temperature

In this section, the body surface temperatures are computed in the time-dependent states. In order to calculate it, it is significant to understand the astrodynamics in orbit because the effective area of the spacecraft during the mission will change over time, depending on the solar position and the orbit period. In this analysis, it is assumed that the solar flux, albedo, and Earth's IR radiations are constant through the mission for each hot and cold case.

The effective area needs to be determined first and it is defined by the beta angle, the orbit period as follows below.

$$T(\beta) = \begin{bmatrix} cos(\beta) & 0 & -sin(\beta) \\ 0 & 1 & 0 \\ sin(\beta) & 0 & cos(\beta) \end{bmatrix}$$

$$T(\theta) = \begin{bmatrix} cos(\theta) & -sin(\theta) & 0 \\ sin(\theta) & cos(\theta) & 0 \\ 0 & 0 & 1 \end{bmatrix}$$

$$\hat{s} = T(\beta)T(\theta)[1\ 0\ 0]^T$$

$$A_{eff} = \left[A_x\ A_y\ A_z\right]^T \cdot \hat{s}$$

$\hat{s}$ is the solar vector based on the beta angle and the orbit period over time.

Once the effective area over time is solved, it is plugged into the thermal balance equation shown in II.C.1. Note that the power generated by the electrical components is now time-dependent. The power budget is calculated by the EPS team and referred from EPS100.

The power usages in the orbit timeline for the hot and cold cases are shown in figure 10. However, the power budget needs to be up to date.

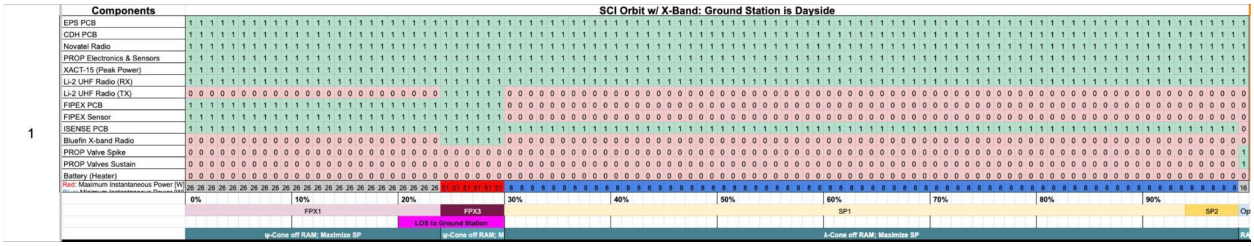

(a) Timeline 1 Power Budget for Hot Case

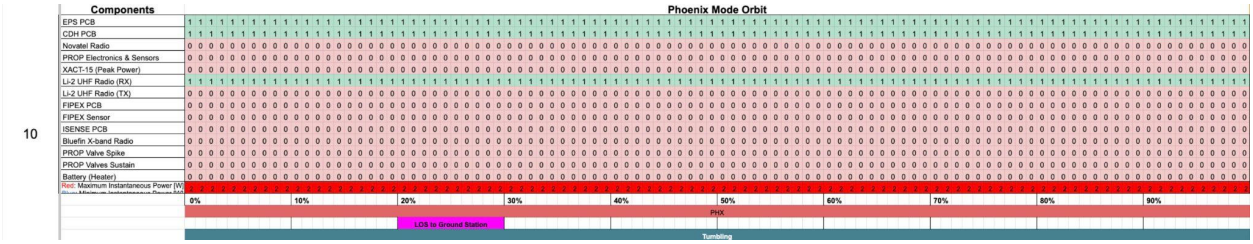

(b) Timeline 10 Power Budget for Cold Case

Figure 10. Power Usage in Orbit Timeline

4. Time-Dependent Component Temperature

In this section, we extend the steady-state analysis by calculating time-dependent temperature variations of spacecraft electrical components throughout the orbit. The same fundamental approach and assumptions from the steady-state model were applied here, with additional consideration of orbital dynamics and power fluctuations over time.

- The analysis uses a lumped-capacitance thermal model, accounting for:
  - Transient heat accumulation
  - Time-varying internal power dissipation
  - Radiative and conductive heat exchange with the structure and space
- The orbit period, eclipse durations, and solar position (via β angle) were used to model heating and cooling intervals.
  Thermal properties such as mass, specific heat, and emissivity for each component were included.
- External boundary conditions (Ts) are derived from Section II.C.3 (Time-Dependent Body Temperature).
- Internal power input profiles for each component were taken from the EPS team's time-based power budget for hot and cold cases.
- Conductive paths (screws, springs, rails) and radiation parameters are modeled identically to the steady-state case.
- MATLAB code was developed to simulate temperature evolution over time, solving Results and Plots.

- Maximum and minimum temperatures were taken into account and repeated the same calculations for electrical components.

IV. Results

A. Steady State Body Surface Temperature

	Hot Case	**Cold Case**
Q_{solar} [W]	1.71	0
Q_{albedo} [W]	4.29	0
Q_{IR} [W]	1.15	0.90
Q_{gen} [W]	30	5
Total Q_{in} [W]	37.15	5.90

Table 8. Input Energy for Hot and Cold Cases

	Hot Case	**Cold Case**
Temperature [C˚]	70.2	-56.4

Table 9. Maximum and Minimum Steady State Surface Temperatures

B. Steady State Component Temperature

Steady-state temperature values were computed using a custom MATLAB script, and the results are summarized in the table below:

Component	**Hot Case [K]**	**Cold Case [K]**	**Hot Case [°C]**	**Cold Case [°C]**
GPS	325.00	221.27	51.85	-51.88
Li Radio	325.07	220.02	51.92	-53.14
Bluefin	320.87	242.07	47.72	-31.08
Battery	320.82	241.45	47.67	-31.70
EPS1	314.78	217.96	41.63	-55.19

EPS2	314.33	217.65	41.18	-55.50
CDH	314.41	217.65	41.26	-55.50
ISENSE2	310.35	258.74	37.21	-14.41
ISENSE1	306.07	256.82	32.92	-16.33
Fipex	319.33	219.24	46.18	-53.91
Fipex Sensor	321.59	220.00	48.44	-53.15
GPS Antenna	321.97	219.72	48.82	-53.43
X-Band	323.61	219.86	50.46	-53.29
ADCS	324.20	219.89	51.05	-53.26
Propulsion	324.46	219.84	51.32	-53.31
Sun Sensor	323.88	220.76	50.73	-52.39
UHF	324.98	220.02	51.83	-53.13

Table 10. Steady State Component Temperature Profile

C. Time-Dependent Body Surface Temperature

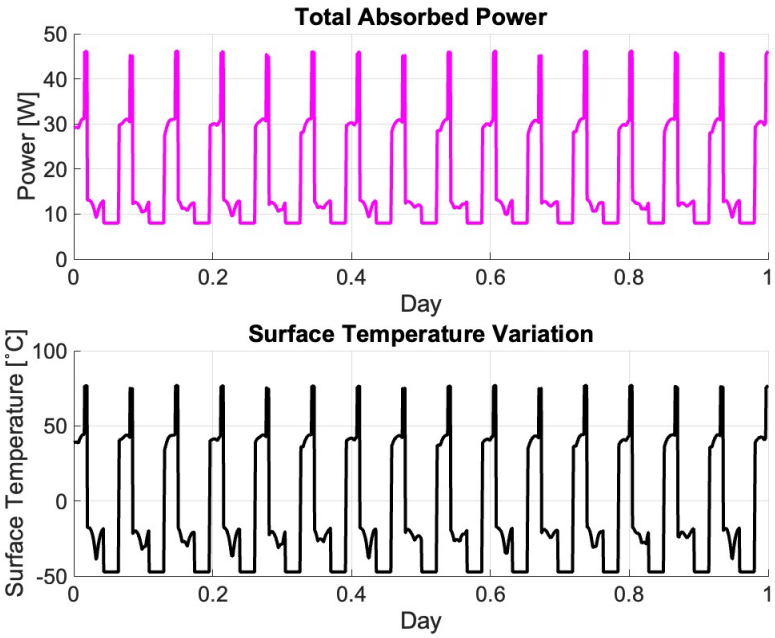

Figure 11. Total Absorbed Power and Surface Temperature Variation for Hot Case

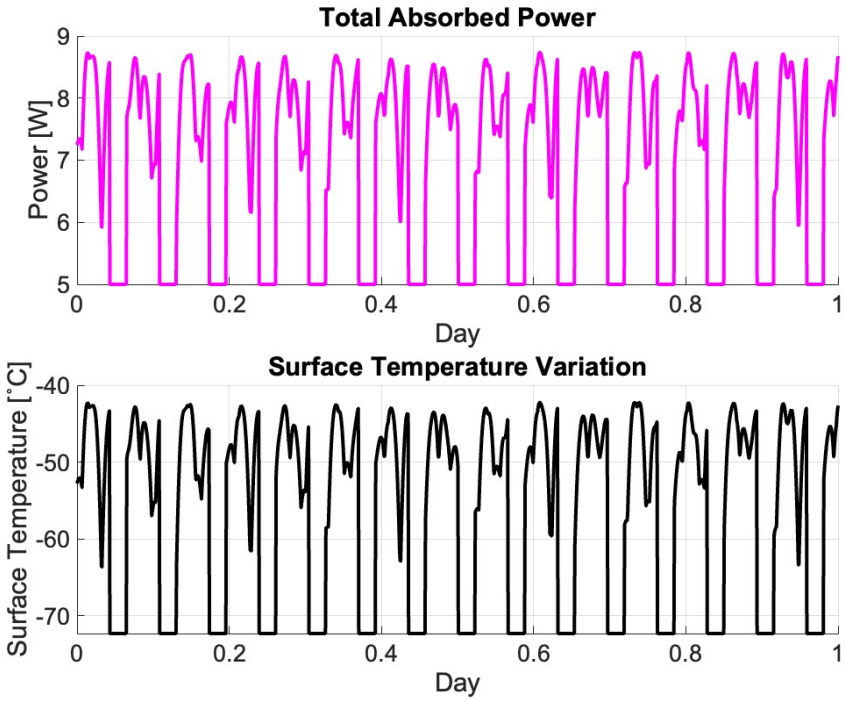

Figure 12. Total Absorbed Power and Surface Temperature Variation for Cold Case

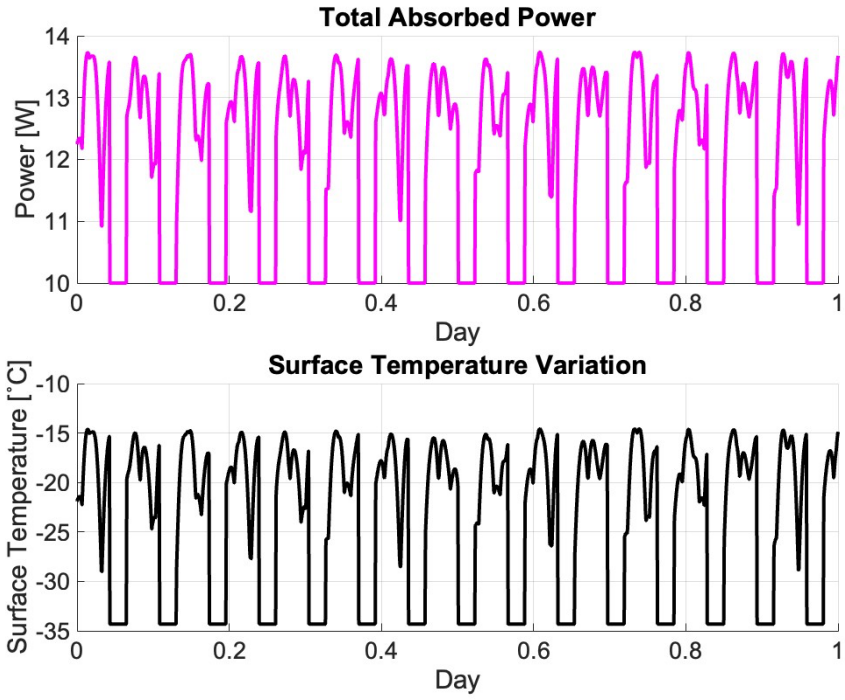

Figure 13. Total Absorbed Power and Surface Temperature Variation with Heater for Cold Case

	Maximum [˚C]	Minimum [˚C]
Hot Case	76.9	-47.3
Cold Case	-42.3	-72.3
Cold Case with Heater	-14.6	-47.3

Table 11. Maximum and Minimum Temperature for Each Case

D. Time-Dependent Component Temperature

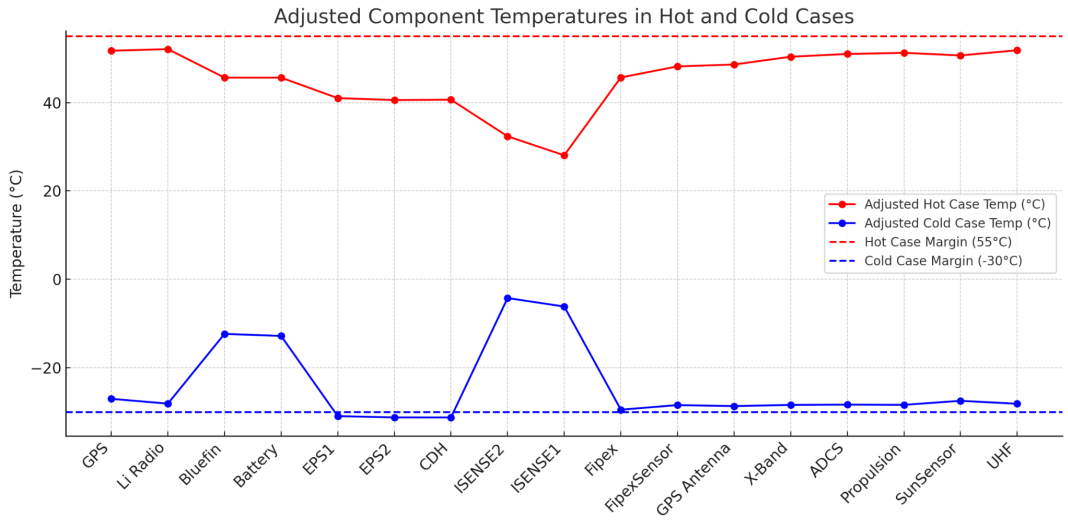

Figure 14.

V. Analysis and Discussion

The mathematical thermal modeling conducted in this analysis provides insight into the expected thermal behavior of the SWARM-EX CubeSat, under both steady-state and time-dependent conditions. The results show a clear difference between idealized steady-state scenarios and realistic transient thermal behavior experienced in orbit.

In the steady-state model, we used high-end values for structure temperatures (70.2 °C for the hot case and −56.4 °C for the cold case). These were derived from a simplified model assuming uniform heating and maximal exposure to incident radiation. As a result, the component-level temperatures calculated under these assumptions were relatively high. However, when compared with the previous semester's Thermal Desktop (TD) simulations, the results remained within a ±10 °C margin, suggesting our mathematical model maintains reasonable accuracy.

Notably, the elevated steady-state temperatures are a product of assuming a conservative heat flux model, maximal absorbed radiation, and a high structural reference temperature, which amplified the thermal load on each component. Nevertheless, these assumptions are helpful in bounding the upper and lower extremes of system performance and highlight potential risks under worst-case conditions. In the transient thermal analysis, more realistic orbit conditions were modeled, including solar flux variation and time-varying internal power based on EPS-provided duty cycles. These time-domain simulations yielded higher peak temperatures in the hot case, largely due to sustained sunlight exposure (e.g., $\beta = 75.3°$) and high duty cycle power inputs. The cold case transient results, on the other hand, showed significant improvement, with component temperatures rising closer to survivable margins due to intermittent exposure and internal heating contributions.

An important observation is the role of thermal contact modeling. By incorporating realistic contact conductance values—through surface areas, fastener materials, and mechanical preload—we found that the conduction paths significantly impact component temperatures. Screws, rails, and springs act as crucial thermal bridges, and their design (material, geometry, preload) has a measurable influence. Similarly, radiative coupling between adjacent components (e.g., GPS and Li Radio) and to space also strongly shapes the thermal profile. These results underscore that improvements in thermal interface materials, fastener configuration, and surface coatings (for better emissivity/absorptivity tuning) can shift the temperature profiles to safer operating conditions. Furthermore, lowering the main structure temperature—either by improved radiator design or better thermal isolation—can result in cooler downstream component temperatures, pushing them well within qualification margins.

VI. Conclusion

This analysis successfully developed and applied a mathematical thermal model to evaluate both steady-state and transient component temperatures in the SWARM-EX CubeSat. Despite a simplified approach for main structure temperature estimation, the component-level results remained consistent with previously validated TD simulations within a ±10 °C range. This validates the utility of the current model for early design-phase assessment and rapid sensitivity evaluations.

Transient analysis further reinforced that cold-case survivability is within acceptable margins, especially with minor thermal design optimizations. However, hot-case temperatures remain on the higher end, suggesting the need for additional radiator optimization or enhanced conductive pathways.

VII. Future Work

1. In this analysis, the view factors for heat radiation were assumed to be 0.5. However, for more precise results, it is necessary to calculate the view factors individually. Each surface of the body (+X, -X, +Y, -Y, +Z, -Z) has a different view factor, which should be considered for a more robust thermal analysis.
2. The body surface temperatures were calculated as a single entity. However, since the 3U CubeSat is a three-dimensional rigid body, each surface (+X, -X, +Y, -Y, +Z, -Z) would realistically experience different heat radiation conditions. In this analysis, heat distribution was assumed to be uniform across all surfaces, resulting in the same temperature profile for every direction.
3. The active battery heater was not considered in this analysis due to limited information, such as its activation timing, specific power usage, and operational characteristics. For future analyses, it will be necessary to collect the battery heater datasheet and incorporate its effects into the thermal model.
4. The spacecraft was assumed to remain in a static orientation throughout the mission, which does not reflect actual operational conditions. In practice, the spacecraft undergoes different attitude modes, such as tumbling and advanced attitude control during the OGNC and SCI orbit phases. For example, advanced pointing scenarios may include a 30˚ cone off the zenith direction or a 30˚ cone off the ram direction. These attitude variations can slightly influence the thermal environment and may impact whether the spacecraft approaches or exceeds critical temperature limits. Therefore, future analyses should account for these dynamic attitude profiles to improve thermal modeling accuracy.

VIII. References

[1] Rickman, S. L. (n.d.). *Introduction to Orbital Mechanics and Spacecraft Attitudes for Thermal Engineers*. NASA.https://tfaws.nasa.gov/wp-content/uploads/Rickman-Presentation.pdf

[2] NASA. (2023). *State-of-the-Art of Small Spacecraft Technology: Thermal Control*. NASA Small Spacecraft Systems Virtual Institute. https://www.nasa.gov/smallsat-institute/sst-soa/thermal-control/

[3] Square Widget. (n.d.). *Solar Coordinates Calculator*. Retrieved April 25, 2025, from https://squarewidget.com/solar-coordinates/

[4] Gilmore, D. G. (Ed.). (2002). *Spacecraft Thermal Control Handbook: Volume I, Fundamental Technologies* (2nd ed.). The Aerospace Press.

[5] Çengel, Yunus A., John M. Cimbala, and Robert H. Turner. *Fundamentals of Thermal-Fluid Sciences*. 5th ed., McGraw-Hill Education, 2017.